Received 5 March 2025, accepted 24 March 2025, date of publication 28 March 2025, date of current version 9 April 2025.
Digital Object Identifier 10.1109/ACCESS.2025.3555935

RESEARCH ARTICLE

Voltage Stability Assessment Through Modal Analysis Using a Smooth Formulation of the Power Flow Problem Based on Sigmoid Functions

JOÃO PEDRO PETERS BARBOSA[1,2], (Graduate Student Member, IEEE), JOÃO ALBERTO PASSOS FILHO[2], (Senior Member, IEEE), RODRIGO ANDRADE RAMOS[1], (Senior Member, IEEE), AND LUÍS FERNANDO COSTA ALBERTO[1], (Senior Member, IEEE)
[1]Department of Computation and Electrical Energy, São Carlos School of Engineering (EESC), University of São Paulo (USP), São Carlos 13566-590, Brazil
[2]Department of Electrical Energy, Federal University of Juiz de Fora (UFJF), Juiz de Fora 36036-900, Brazil

Corresponding author: João Alberto Passos Filho (joao.passos@ufjf.br)

This work was supported by the National Research Council (CNPq), Brazilian Federal Agency for Support and Evaluation of Graduate Education (CAPES), State of Minas Gerais Research Foundation (FAPEMIG), Federal University of Juiz de Fora (UFJF), National Institute of Science and Technology in of Electric Energy (INERGE), and São Paulo Research Foundation (FAPESP) under Grant 2018/20104-9.

ABSTRACT This paper introduces a voltage stability analysis based on an innovative formulation of the power flow problem designed to address and eliminate discontinuities associated with reactive power limits from synchronous generators, synchronous compensators, and static VAr compensators. By replacing these discontinuities with appropriately tuned sigmoid functions, we achieve smooth behavior without compromising accuracy. A key advantage of this formulation is its ability to convert limit-induced bifurcations into saddle-node bifurcations. This conversion allows the voltage security studies to focus solely on identifying saddle-node bifurcations, leading to significant computational efficiency. In the present context of modern power systems, characterized by growing demand and uncertainties in generation capacity, this new approach is relevant for ensuring the computational feasibility of highly uncertain scenarios. The effectiveness of the proposed formulation is validated using a modal analysis of the reduced Jacobian matrix, which focuses mainly on the smooth control equations incorporated into the solution of the problem using Newton's method. Our findings are substantiated by simulations on four test systems, including the IEEE 118-Bus system, which shows the conversion process of bifurcations as described. The results presented validate and indicate the effectiveness of the proposed technique.

INDEX TERMS Voltage stability, continuation power flow, bifurcations, reactive power limits, modal analysis.

I. INTRODUCTION

Electrical Power Systems (EPS) are complex networks comprising various components such as generators, loads, transformers, and transmission lines among others. Each equipment has unique operational characteristics that necessitate specific control actions to maintain reliable and efficient operation. The Power Flow (PF) calculation [1] is one of the most significant tools for EPS analyses, and accurately modeling these control actions is crucial for precise results.

As the energy transition progresses, leading to an increased integration of intermittent power sources replacing traditional technologies, the level of uncertainty in EPS operation continues to rise [2]. Consequently, there is a frequent need for the recurrent calculation of multiple PF solutions given the wide range of possible scenarios. This necessity highlights the growing importance of developing more computationally

The associate editor coordinating the review of this manuscript and approving it for publication was Emilio Barocio.

efficient PF formulations and solution methods. Recent research underscores the relevance of this topic, as seen in studies focused on improving PF efficiency and reliability [3], [4], [5].

Stability and security are two important features to analyze in EPS operation and planning environments. As defined in [6], EPS stability refers to the ability of a system to reach an equilibrium condition after a disturbance, with its variables bounded to maintain system integrity. Recent work defines stability as encompassing not only angle, frequency, and voltage stability [6] but also resonance and converter-driven stability [7]. In particular, maintaining stability as the load increases is a typical objective of voltage stability analyses and is directly related to the ability of the EPS to provide reactive power support.

Static formulations for voltage stability studies [8], [9], [10] are often based on continuous power flow formulations and direct methods formulations [11], [12]. Regarding the Continuation Power Flow (CPF) [13], it applies successive PF calculations considering arbitrary load growth direction and synchronous generation redispatch, while still maintaining the accuracy of the models of EPS components and their respective control actions. The paper [14] discusses the significance of load modeling aspects related to demand response in the context of voltage stability studies, emphasizing the role of grid reactive power behavior in this type of analysis.

One significant challenge associated with this formulation is achieving the EPS point of maximum loadability while considering the reactive power limits of equipment such as synchronous generators (SGs), synchronous condensers (SCs), and static VAr compensators (SVCs). In most PF and CPF simulations, these limits introduce discontinuities into the models, typically handled using heuristic procedures by bus-type switching [15]. Managing these discontinuities results in a loss of computational efficiency, as it necessitates recalculating an entire step of the solution process whenever a single limit is violated.

Since the EPS voltage stability is directly related to the reactive power support provided by its components, limitations - or discontinuities - in this support may produce instability in the system. Mathematically, this type of instability is associated with a limit-induced bifurcation (LIB), which is quite different from the saddle-node bifurcation (SNB) [8]. While there are efficient techniques to find a SNB in a CPF, the same does not apply to a LIB. Differentiated by a mathematical property, these bifurcation classifications highlight the complexity of voltage collapse analysis.

To address this challenge, recent research has introduced a novel Power Flow (PF) formulation approach known as Smooth Power Flow (SPF) [16], [17]. This innovative method aims to enhance power system analysis by converting all static bifurcations into SNBs. Although SPF does not prevent voltage collapse, it significantly simplifies the identification of its conditions and causes, thereby improving the overall efficiency and reliability of power system stability assessments. On the other hand, the paper [18] presents the formulation and convexification of voltage stability-constrained optimal power flow (VSC-OPF), integrating PV-PQ switching to co-optimize generation dispatch and bus type configuration.

Motivation and Contribution of This Work: Given the background, this paper uses an SPF approach based on [16] by employing appropriately parameterized sigmoid functions to approximate the discontinuous behavior of equipment due to reactive power limits. The result is a smooth formulation of the traditional PF problem, enhancing the computational efficiency of PF solution calculations. This work demonstrates, as a main contribution, that the smoothed formulation based on sigmoid functions [19] converts LIBs into SNBs, allowing the application of well-established computational techniques to identify SNBs close enough to LIBs. This dual benefit not only simplifies the computation process but also enhances computational efficiency.

Furthermore, this work advances the field by numerically demonstrating and identifying SNBs in the SPF formulation. This is achieved through the implementation of modal analysis [20], which provides enhanced insights into voltage instability events in EPSs. The results are validated by simulations of 4 test systems, including the IEEE 118-Bus system, highlighting the mentioned bifurcation conversion.

This paper is organized as follows: Section II reviews the main concepts of the SPF formulation, with main focus on voltage stability analysis. In Section III, the smooth methodologies for modeling reactive power limits from SGs, SCs, and SVCs are introduced. Section IV presents the simulation results. Lastly, Section V presents the main conclusions regarding the work and results obtained.

II. SMOOTH POWER FLOW

The SPF formulation represents a recent research approach within the PF domain. The central premise of this methodology lies in smoothing out electric devices' operational limits, as its goal is to enhance the voltage stability analysis in power systems. Consequently, a novel formulation process is embraced for the system of inequalities, which is then integrated into the established PF framework.

A pivotal advancement in this field was made by [17], which not only established a robust mathematical foundation for the Smooth Power Flow (SPF) formulation but also introduced significant contributions to the literature on voltage stability. This work encompasses the modeling of diverse electrical device control and operational constraints and proposes new techniques for contingency prioritization and Voltage Stability Margin (VSM) assessment using the SPF approach, thereby enriching the existing methodologies and enhancing the understanding of voltage stability.

The proposed idea of smoothing out the operational limits of electrical equipment was initially investigated by [21], which dealt with modeling reactive power generation constraints using hyperbolic or sigmoid functions, proposing the transformation of an "undifferentiable" condition into a "differentiable" one. Similarly, [19] presented a comparable methodology for reactive power limits, introducing the use of sigmoid-based switches to model synchronous generator behavior. The conclusion drawn was that conventional bus re-specification (PV to PQ and vice-versa) is unnecessary, and a small number of iterations still sufficed for power flow convergence, with no commitment to solution precision. In a recent study, [22] applies the SPF reactive power generation limit model to evaluate power flow accuracy and load margin computation based on bus-type switching. This study introduced two smooth functions and analyzed multiple power flow solutions using varying PV to PQ switching strategies.

In [23], a new methodology for reactive power limits using the smooth model to rapidly identify LIBs arising from violations of reactive power constraints was proposed. Building on this foundation, [24] explored the methodology, further deducing novel voltage stability indices by accounting for uncertainties in loading parameters. Subsequent works by [16] proposed various SPF models for distinct electric devices, approximating their "control limits and saturation effects". Moreover, these works demonstrated that traditional static bifurcations from PF simulations translate into SNBs within the SPF formulation. This advancement is then leveraged for estimating load margin in contingency assessment and ranking for voltage stability analysis.

In this context, in the proposed methodology sigmoid functions are utilized for modeling the operational limits of SGs and SVCs. The methodology pioneered by [19] and mathematically supported by [17] is adopted for modeling these electric devices, given a specific emphasis on voltage stability analysis. Integrating smooth functions into traditional PF formulation leads to the conversion of LIBs into corresponding SNBs. This transition holds the potential for substantial enhancements in Voltage Stability Assessment (VSA), as elaborated in this work. The proposed incorporation adopts a *full* Newton methodology, integrating the control equations into the set of algebraic power equations within the PF problem. This comprehensive approach ensures a more robust and accurate solution by simultaneously solving for power flows and control variables.

The continuation power flow formulation stands out among the existing simulation tools capable of evaluating power systems' voltage stability in terms of load demand increments and synchronous generation redispatch. By means of CPF, it is possible to analyze voltage collapse scenarios for EPSs, which are classified as SNB, LIB, or others. Considering the conventional PF formulation, SNBs are identified through the singularity and eigenvalue analysis of the Jacobian matrix. However, the same does not prevail for voltage collapse scenarios classified as LIBs, once they cannot be studied using eigenvalue analysis since they are characterized by changes in the CPF formulation, which, in turn, require modifications in the Jacobian matrix of the PF problem.

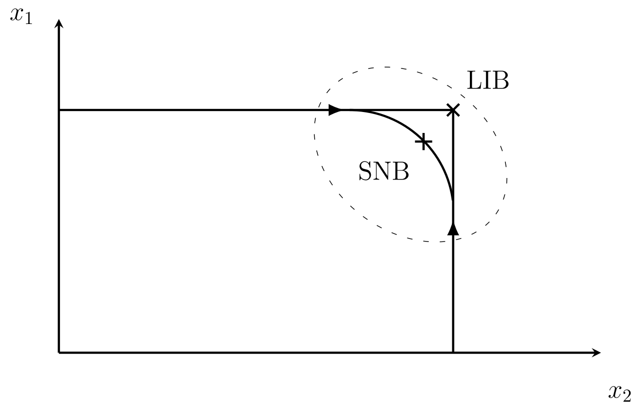

FIGURE 1. SPF identification of SNB arbitrarily close to LIB. Adapted from [17].

In [17], considering the SPF formulation, it was mathematically proven the existence of a SNB of the smoothed system corresponding to the LIB of the original system. Figure 1 illustrates this condition, where there is a SNB arbitrarily close to a LIB. The dashed lines delimit an arbitrarily close region where both bifurcation points are close to each other. Although there are no established methods for proving the proximity of a region or how close a SNB is to a LIB, this paper provides a numerical demonstration of SNBs being close to LIBs.

Due to the smoothness of the SPF formulation, which approximates the discontinuities of electric devices' operational limits, a LIB can be accurately represented as a SNB. In the SPF formulation, all bifurcations in the CPF problem are converted to SNBs, allowing the use of modal analysis techniques to compute the eigenvalues related to voltage collapse. This makes it easier to identify the system elements involved in the voltage stability problem of EPS.

III. SMOOTHED POWER FLOW FORMULATION

The methodology assumed in this paper is detailed in the subsequent sections, where sigmoid functions are employed to introduce smoothness into the modeling of reactive power limits for SGs, SCs and SVCs.

A. SIGMOID FUNCTION

The sigmoid function equation is defined by:

$$sig(x) = \frac{1}{1 + e^{-slp \cdot (x - lim)}} \tag{1}$$

where x is the input variable, slp is the slope variable and lim is the inflection point variable. The function typically produces an output within the range of 0 to 1. As the slope variable increases, the curve inclination becomes steeper, approaching the behavior of a step function. This characteristic offers advantages in modeling inequalities related to the operational limits of electrical devices, as smooth step functions help mitigate discontinuity issues commonly encountered in traditional power flow formulations.

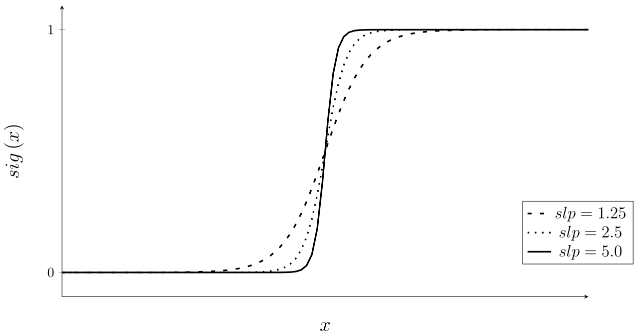

FIGURE 2. Sigmoid function slope variation. Adapted from [25].

The sigmoid functions, therefore, are set to be implemented in the static modeling of electric devices' operational limits by an association with control equations following the mathematical logic of truth tables. Since the high slope value approximates the operation of the sigmoid function as that of a switch, the sigmoid function can be considered a logical variable. The switches are arranged to control equations that model electric devices' operational limits and, consequently, are combined together into one equivalent control equation.

B. SYNCHRONOUS GENERATORS

Four sigmoid switches are employed for the static smooth modeling of SGs reactive power generation limit, according to [19]. The sigmoid switching equations are expressed in terms of the reactive power generated ($Q_{G_k,\,gen}$), detailed in Equations (2) and (3), and their own bus voltage magnitude ($V_{k,\,gen}$), detailed in Equations (4) and (5).

$$sw1 = \frac{1}{1 + e^{-slp\cdot\left(Q_{G_k,\,gen} - lim_q^{sup}\right)}} \tag{2}$$

$$sw2 = \frac{1}{1 + e^{+slp\cdot\left(Q_{G_k,\,gen} - lim_q^{inf}\right)}} \tag{3}$$

$$sw3 = \frac{1}{1 + e^{+slp\cdot\left(V_{k,\,gen} - lim_v^{sup}\right)}} \tag{4}$$

$$sw4 = \frac{1}{1 + e^{-slp\cdot\left(V_{k,\,gen} - lim_v^{inf}\right)}} \tag{5}$$

where:

- $lim_q^{sup} = Q_{G_k,\,gen}^{max} - tol_q$
- $lim_q^{inf} = Q_{G_k,\,gen}^{min} - tol_q$
- $lim_v^{sup} = V_{k,\,gen}^{ref} - tol_v$
- $lim_v^{inf} = V_{k,\,gen}^{ref} - tol_v$
- tol_q and tol_v are small constants.

In (6), the sigmoid switches are associated with the synchronous generator control equations that best represent the equipment's operative states. This equation is linearized and incorporated into the Jacobian matrix, considering $Q_{G_k,\,gen}$ as new power flow state variable. Table 1 describes the control equation (6) residue for each operational state of the smooth modeling of SGs. The symbol "×" visible in Table 1 corresponds to a non-interfering value of sigmoid switches in the overall output result.

TABLE 1. SGs sigmoid switches operation and control equation output.

Operational State	$sw1$	$sw2$	$sw3$	$sw4$	Δy
Superior Limit Violation	1	0	1	×	$Q_{G_k,\,gen}^{max} - Q_{G_k,\,gen}$
Normal	1	0	0	×	$V_{k,\,gen}^{ref} - V_{k,\,gen}$
	0	0	×	×	
	0	1	×	0	
Inferior Limit Violation	0	1	×	1	$Q_{G_k,\,gen}^{min} - Q_{G_k,\,gen}$

$$\begin{aligned} y = {} & (sw1\cdot sw3)\cdot(1 - sw2\cdot sw4)\cdot\left(Q_{G_k,\,gen} - Q_{G_k,\,gen}^{max}\right)\cdots \\ & + (1 - sw1\cdot sw3)\cdot(1 - sw2\cdot sw4)\cdot\left(V_{k,\,gen} - V_{k,\,gen}^{ref}\right)\cdots \\ & + (1 - sw1\cdot sw3)\cdot(sw2\cdot sw4)\cdot\left(Q_{G_k,\,gen} - Q_{G_k,\,gen}^{min}\right) \end{aligned} \tag{6}$$

C. STATIC VAr COMPENSATOR

Similarly, as presented in subsection III-B, two sigmoid switches are employed for the static smooth modeling of SVCs reactive power generation capacity limit. The sigmoid switching equations are expressed in terms of the controlled bus voltage magnitude ($V_{m,\,svc}$), as detailed in Equations (7) and (8).

$$sw5 = \frac{1}{1 + e^{-slp\cdot\left(V_{m,\,svc} - lim_v^{sup}\right)}} \tag{7}$$

$$sw6 = \frac{1}{1 + e^{+slp\cdot\left(V_{m,\,svc} - lim_v^{inf}\right)}} \tag{8}$$

where:

- $lim_v^{sup} = V_{m,\,svc}^{ref} + r\cdot B_{svc}^{min}\cdot V_{k,\,svc}^2 + tol_v$
- $lim_v^{inf} = V_{m,\,svc}^{ref} + r\cdot B_{svc}^{max}\cdot V_{k,\,svc}^2 - tol_v$
- tol_v is a small constant

The equations that define the upper and lower voltage magnitude limit variables, along with the control equations governing the steady-state behavior of the SVC (9) [10], are formulated based on the relationship between the reactive power generated by the equipment and the voltage magnitude of the controlled bus, as depicted in Figure 3. The *droop* parameter, denoted by "r," determines the variation in the controlled bus voltage magnitude when the SVC operates within its linear region. Table 2 describes the control equation (9) residue for each operational state of the smooth modeling of SVCs.

$$\begin{aligned} y = {} & sw5\cdot\left(Q_{G_k,\,svc} - V_{k,\,svc}^2\cdot B_{svc}^{min}\right)\cdots \\ & + sw6\cdot\left(Q_{G_k,\,svc} - V_{k,\,svc}^2\cdot B_{svc}^{max}\right)\cdots \\ & + \ (1 - sw5)\cdot(1 - sw6) \\ & \cdot\left(V_{m,\,svc} - V_{m,\,svc}^{ref} - r\cdot Q_{G_k,\,svc}\right) \end{aligned} \tag{9}$$

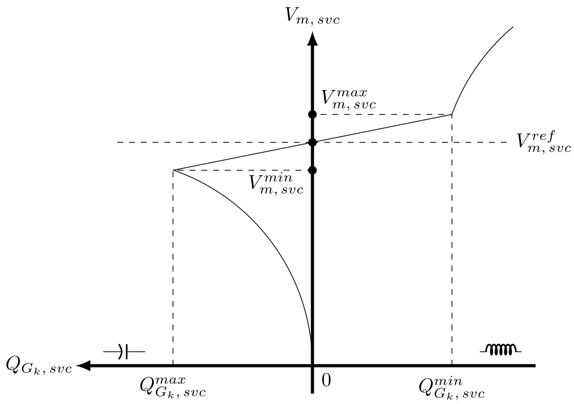

FIGURE 3. SVC reactive power generation per controlled bus voltage magnitude characteristic. Adapted from [25].

TABLE 2. SPF-SVC reactive power injection methodology sigmoid switches operation and control equation residue output.

Operational Region	$sw5$	$sw6$	Δy
Inductive	1	0	$V_{k,\,svc}^2 \cdot B_{svc}^{min} - Q_{G_k,\,svc}$
Linear	0	0	$V_{m,\,svc}^{ref} + r \cdot Q_{G_k,\,svc} - V_{m,\,svc}$
Capacitive	0	1	$V_{k,\,svc}^2 \cdot B_{svc}^{max} - Q_{G_k,\,svc}$

D. FULL NEWTON METHOD

The power equations that model an EPS are synthesized by (10), according to [10]:

$$\boldsymbol{g}\left(\boldsymbol{\theta}, \boldsymbol{V}\right) = \boldsymbol{0} \tag{10}$$

where $\boldsymbol{g}$ is the set of algebraic power equations, $\boldsymbol{\theta}$ is the bus phase angle vector, and $\boldsymbol{V}$ is the bus voltage magnitude vector. Considering a *full* Newton implementation, the smooth control equations and control variables, as proposed in (6) and (9), are incorporated into the set of algebraic equations:

$$\boldsymbol{g}\left(\boldsymbol{\theta}, \boldsymbol{V}, \boldsymbol{x}\right) = \boldsymbol{0} \tag{11}$$

where $\boldsymbol{x}$ is the control variable vector, which dimension depends directly on the number of control equations $\boldsymbol{y}$ incorporated in the power flow problem. In applying Newton-Raphson's numerical method, an initial estimation for θ, V, and x is made and the corresponding system of algebraic equations (11) is linearized, resulting in the following:

$$\boldsymbol{\Delta g} = \boldsymbol{J} \cdot \boldsymbol{\Delta X} \tag{12}$$

$$\begin{bmatrix} \boldsymbol{\Delta P} \\ \boldsymbol{\Delta Q} \\ \Delta \boldsymbol{y} \end{bmatrix} = \underbrace{\begin{bmatrix} \partial \boldsymbol{P}/\partial \boldsymbol{\theta} & \partial \boldsymbol{P}/\partial \boldsymbol{V} & \partial \boldsymbol{P}/\partial \boldsymbol{x} \\ \partial \boldsymbol{Q}/\partial \boldsymbol{\theta} & \partial \boldsymbol{Q}/\partial \boldsymbol{V} & \partial \boldsymbol{Q}/\partial \boldsymbol{x} \\ \partial \boldsymbol{y}/\partial \boldsymbol{\theta} & \partial \boldsymbol{y}/\partial \boldsymbol{V} & \partial \boldsymbol{y}/\partial \boldsymbol{x} \end{bmatrix}}_{\boldsymbol{J}} \cdot \begin{bmatrix} \boldsymbol{\Delta \theta} \\ \boldsymbol{\Delta V} \\ \boldsymbol{\Delta x} \end{bmatrix} \tag{13}$$

where:

$$\boldsymbol{\Delta P} = \boldsymbol{P}^{sch} - \boldsymbol{P}^{cal} \tag{14}$$
$$\boldsymbol{\Delta Q} = \boldsymbol{Q}^{sch} - \boldsymbol{Q}^{cal} \tag{15}$$
$$\boldsymbol{\Delta y} = \boldsymbol{y}^{sch} - \boldsymbol{y}^{cal} \tag{16}$$
$$P_k^{cal}\left(\boldsymbol{\theta}, \boldsymbol{V}\right) = V_k \cdot \sum_{m \in \Omega_k} V_m \cdot \left(G_{km}\cos\theta_{km} + B_{km}\sin\theta_{km}\right) \tag{17}$$
$$Q_k^{cal}\left(\boldsymbol{\theta}, \boldsymbol{V}\right) = V_k \cdot \sum_{m \in \Omega_k} V_m \cdot \left(G_{km}\sin\theta_{km} - B_{km}\cos\theta_{km}\right) \tag{18}$$

In above equations, *sch* and *cal* denote scheduled and calculated (at every iteration) variables. $\boldsymbol{\Delta g}$ is the vector of power equations variation, $\boldsymbol{J}$ is referred as Jacobian matrix, and $\boldsymbol{\Delta X}$ is the vector of state and control variables variation.

Given the smooth modeling of control equations for synchronous generators (SGs) and static var compensators (SVCs), modal analysis is applied using a reduced form of the Jacobian matrix (13) [10], [20], [26]. This approach reveals the relationship between the smooth control equations and the voltage magnitude state variables, especially as the power system approaches collapse.

E. MODAL ANALYSIS

The modal analysis is implemented for numerical verification of SNBs close to LIBs, as the eigenvalues and eigenvectors will be extracted from the proposed *full* Newton Jacobian matrix (13), in its reduced form defined as $\boldsymbol{J_R}$ [10], [20], [26]. The eigenvalues will identify the interaction modes between reactive power limits control equations, whereas the eigenvectors fill in sensitive information regarding the eigenvalues controllability and observability [27].

$$\boldsymbol{\Delta Y} = \boldsymbol{J_R} \cdot \boldsymbol{\Delta X} \tag{19}$$

where:

$$\boldsymbol{J_R} = \left[\boldsymbol{J_{YX}} - \boldsymbol{J_{Y\theta X}} \cdot \boldsymbol{J_{PQ\theta V}}^{-1} \cdot \boldsymbol{J_{PQX}}\right]_{(\mathrm{N_{CTRL}})\times(\mathrm{N_{CTRL}})} \tag{20}$$
$$\boldsymbol{J_{YX}} = \left[\, \partial \boldsymbol{y}/\partial \boldsymbol{x} \,\right]_{(\mathrm{N_{CTRL}})\times(\mathrm{N_{CTRL}})} \tag{21}$$
$$\boldsymbol{J_{Y\theta X}} = \left[\, \partial \boldsymbol{y}/\partial \boldsymbol{\theta} \;\; \partial \boldsymbol{y}/\partial \boldsymbol{V} \,\right]_{(\mathrm{N_{CTRL}})\times(2\mathrm{N_{BUS}})} \tag{22}$$
$$\boldsymbol{J_{PQX}} = \begin{bmatrix} \partial \boldsymbol{P}/\partial \boldsymbol{\theta} & \partial \boldsymbol{P}/\partial \boldsymbol{V} \\ \partial \boldsymbol{Q}/\partial \boldsymbol{\theta} & \partial \boldsymbol{Q}/\partial \boldsymbol{V} \end{bmatrix}_{(2\mathrm{N_{BUS}})\times(2\mathrm{N_{BUS}})} \tag{23}$$
$$\boldsymbol{J_{PQX}} = \begin{bmatrix} \partial \boldsymbol{P}/\partial \boldsymbol{x} \\ \partial \boldsymbol{Q}/\partial \boldsymbol{x} \end{bmatrix}_{(2\mathrm{N_{BUS}})\times(\mathrm{N_{CTRL}})} \tag{24}$$

The reduced Jacobian matrix dimension in (20) depends only on the amount of control equations (N_{CTRL}) that are incorporated into the set of algebraic power equations. As a result, it is particularly analyzed the correlation between reactive power limits and voltage magnitude for EPS. N_{BUS} is the number of buses in the system.

Since only the control equations are being analyzed in the modal analysis, it could be observed that all SNB bifurcations encountered during simulations resulted from them. This analysis is valid once that the SPF formulation smoothness is introduced precisely by the control equations incorporated into the Jacobian matrix.

The modal analysis properties presented in [20] will be implemented onto the reduced Jacobian matrix, and the sensitivity between a SG or SVC reactive power generation and voltage magnitude at bus k will be evaluated as follows:

$$\frac{\partial Q_{G_k,\,gen}}{\partial V_{k,\,gen}} = \sum_{i=1}^{\mathrm{N}_{BUS}+\mathrm{N}_{CTRL}} \phi_{ki} \cdot \lambda_i^{eig} \cdot \psi_{ik} \tag{25}$$

Within the modal analysis, the goal is to identify which generator is associated with critical eigenvalue via modal-shape and participation factor analyzes. The critical eigenvalue are responsible for the Jacobian matrix singularity, therefore characterizing a voltage collapse classified as SNB.

IV. SIMULATION RESULTS

This section presents the simulation results for the proposed smooth static modeling of SGs, SCs, and SVCs reactive power limits in the power flow analysis. The CPF [13] is used for the assessment of voltage stability, incorporating small increments of load that lead to voltage collapse scenarios. All case studies analyze voltage collapse scenarios initially classified as LIB, considering SGs and SVCs with non-smooth static modeling. However, when applying the proposed smooth modeling technique, a transformation of the voltage collapse point classification from LIB to SNB is observed and verified using modal analysis [20].

In the simulations, regarding the CPF results, $\lambda = 0$ corresponds to the base case power flow solution. A load increment with respect to the base case load power factor is adopted in conjunction with generation redispatch of SGs. The eigenvalues of the modal analysis are computed at the maximum loadability point for each case analyzed.

A. SYNCHRONOUS GENERATORS Q-LIMITS

1) TUTORIAL SYSTEM I

The power system topology and data are illustrated in Figure 4. The parameters for the static modeling of synchronous generators (SGs) reactive power limits, using a sigmoid switch function, are provided in Table 3.

The 4-bus tutorial system is a extended version of a single machine infinite-bus (SMIB) system introduced for discussions regarding voltage stability analysis. A high impedance branch is adopted between buses 2 and 3, separating the EPS into two distinct electrical areas. The CPF loading variation was applied only for the PQ bus connected to the slack bus, while the other PQ load remained constant throughout the whole simulation.

As a result of using the CPF a voltage collapse scenario classified as SNB was identified. The details of this collapse are listed in Table 4. The identification of an eigenvalue close to zero confirms that the system reaches a voltage collapse scenario due to the reactive power limitations of the slack bus generator.

Modal analysis corroborates with the results indicating through the analysis of the participation factor, the synchronous slack bus generator as the main responsible for the collapse. These results are shown in Table 5. In this table, it is possible to verify that the smallest eigenvalue is directly associated with the generator of bus 1. This can be observed through the participation factors calculated for this eigenvalue. It is worth pointing out that if conventional modeling were used, the system's maximum loading point would not be associated with an eigenvalue close to zero. As a result, the issue related to the reactive power generation limit would not be identified.

At the voltage collapse point, the sigmoid switch values of the slack bus synchronous generator, shown in Table 6, indicate a transition from normal mode control to the upper limit violation control mode as the generator reaches its reactive power limit.

TABLE 3. Parameters adopted in the SGs *Q*-Limits smooth modeling for the tutorial system 1 case study.

Sigmoid Switches Slope (slp)	$0.9235 \cdot 10^{14}$
Sigmoid Switches Tolerances ($tol_{q,v}^{sup,inf}$)	10^{-20}

TABLE 4. Tutorial system 1 SNB classification of voltage collapse, considering SGs *Q*-Limits smooth modeling.

Maximum Loadability	1822.121465441%
Voltage Stability Margin	172.2121465441 MW
Reactive Power Generated by $Q_{G,\infty}$	0.649999999999986 p.u.
J_R eigenvalues	[0.00835568031 316.460440]

TABLE 5. Tutorial system 1 modal analysis results.

Eigenvalue (λ^{eig})	Participation Factor
0.00835568031	$Q_{G,\infty}$ = 100%, $Q_{G,PV}$ = 0%
316.460440	$Q_{G,\infty}$ = 0%, $Q_{G,PV}$ = 100%

TABLE 6. Tutorial system 1 slack bus synchronous generator sigmoid switches values at the point of voltage collapse.

$sw1$	$sw2$	$sw3$	$sw4$
0.25	0.00	0.33	0.67

TABLE 7. Parameters adopted in the SGs *Q*-Limits smooth modeling for the IEEE 118-Bus system case study.

Sigmoid Switches Slope (slp)	10^{10}
Sigmoid Switches Tolerances ($tol_q^{sup,inf}$)	10^{-17}
Sigmoid Switches Tolerances ($tol_v^{sup,inf}$)	10^{-8}

2) IEEE 118-Bus SYSTEM

According to previous studies [28], [29], a voltage collapse scenario was reproduced for the IEEE 118-Bus system. This EPS data is available in [30], while the parameters for the sigmoid switch used in the static modeling of synchronous generators' (SGs) reactive power limits are presented in Table 7.

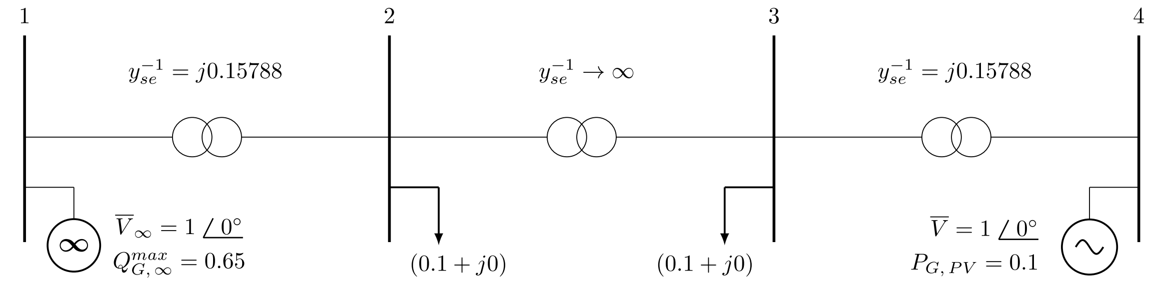

FIGURE 4. Tutorial system 1 topology and bus data. Adapted from [25].

TABLE 8. IEEE 118-Bus SNB classification of voltage collapse, considering SGs *Q*-Limits smooth modeling.

Maximum Loadability	100.7694%
Voltage Stability Margin	3696.221592 MW
Reactive Power Generated by $Q_{G,4}$	2.9999992291 p.u.
J_R eigenvalues	[(...) 0.012667277 0.01390944 0.02319254 0.0277936 0.03126189 (...)]

TABLE 9. IEEE 118-Bus modal analysis results.

Eigenvalue (λ^{eig})	Participation Factor
0.012667277	$Q_{G,116} = 65.2\%, Q_{G,69} = 30.9\%, Q_{G,66} = 3.2\%$
0.01390944	$Q_{G,25} = 55.4\%, Q_{G,26} = 42.3\%, Q_{G,27} = 1.1\%$
0.02319254	$Q_{G,90} = 54.9\%, Q_{G,89} = 39.6\%, Q_{G,91} = 4.5\%$
0.0277936	$Q_{G,4} = 90.2\%, Q_{G,113} = 7.7\%, Q_{G,40} = 1.2\%$
0.03126189	$Q_{G,61} = 76.1\%, Q_{G,54} = 23.6\%$

Using the CPF method, a voltage collapse scenario classified as SNB was detected. This collapse occurs when the synchronous generator at bus 4 reaches its maximum reactive power generation limit. The details regarding this SNB bifurcation are provided in Table 8. Among the five smallest eigenvalues obtained from the matrix $\boldsymbol{J_R}$, only one indicates the synchronous generator responsible for the voltage collapse, whereas the other eigenvalues indicate control conflicts between two or more electrically close SGs. This conclusion is confirmed by the modal analysis results in Table 9, where the eigenvalue most associated with the voltage collapse is highlighted.

Although the highlighted eigenvalue is not the smallest, it has highest participation factor value, indicating that the reactive power generated by the synchronous generator at bus 4 plays a crucial role in the voltage collapse. Additionally, this eigenvalue exhibits the most significant variation in participation factor values. In contrast, the other eigenvalues display more balanced participation factors, suggesting control conflicts among the SGs associated with them [27].

B. STATIC VAr COMPENSATOR Q-LIMITS

The following case studies build upon the work of [31], which investigates voltage collapse scenarios classified as LIB. These scenarios arise due to the reactive power generation limits of SVCs, considering a non-smooth static modeling approach for the control device.

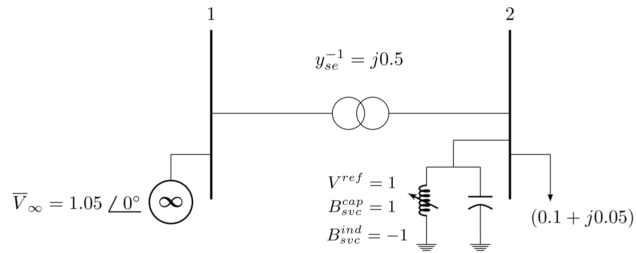

FIGURE 5. Tutorial system 2 topology and data. Adapted from [25].

TABLE 10. Parameters adopted in the SVC *Q*-Limits smooth modeling for the tutorial system 2 case study.

Sigmoid Switches Slope (*slp*)	$0.965 \cdot 10^8$
Sigmoid Switches Tolerances ($tol_v^{sup,inf}$)	10^{-14}

1) TUTORIAL SYSTEM II

The system under study is a SMIB, with its topology and data illustrated in Figure 5. In this setup, a SVC is connected to the infinite bus and is responsible for regulating the voltage magnitude at its own bus to a predefined reference value.

For this case study, the static modeling of the SVC reactive power limits is represented using a sigmoid switch function. The parameters adopted for this modeling approach are detailed in Table 10. The SVC droop is set at 5%.

As a result of the CPF simulation, a voltage collapse scenario was identified and classified as SNB. The collapse occurs when the SVC reaches its maximum reactive power generation limit, as detailed in Table 11. Since the matrix $\boldsymbol{J_R}$ includes a single smooth control equation, only one eigenvalue is analyzed, which corresponds to the SVC. This confirms that the voltage collapse is solely due to the SVC reaching its maximum reactive power limit. Further analysis of the sigmoid switch values at the voltage collapse point, as shown in Table 12, reveals a in-between transition from the normal mode control equation to the upper-limit violation mode control equation, as illustrated in Figure 1.

2) IEEE 30-Bus SYSTEM

Following the work of [31], three SVCs are included in the IEEE 30-Bus system to simulate a voltage collapse scenario.

TABLE 11. Tutorial system 2 SNB classification of voltage collapse, considering SVC *Q*-Limits smooth modeling.

Maximum Loadability	1173.536014%
Voltage Stability Margin	107.35260136855 MW
Reactive Power Generated by $Q_{G_2,\,svc}$	0.910976198541199 p.u.
J_R eigenvalue	[0.00359571]

TABLE 12. Tutorial system 2 SVC sigmoid switches values at the voltage collapse point.

$sw5$	$sw6$
0.00	0.49

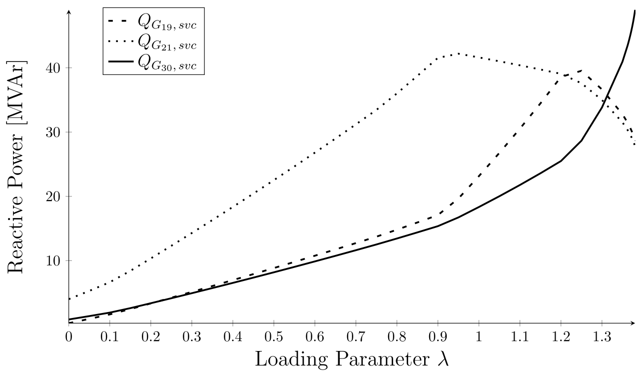

FIGURE 6. IEEE 30-Bus SVCs reactive power generation per network load increment. Adapted from [25].

TABLE 13. SVC parameters in IEEE 30-Bus system.

Bus	V^{ref} [p.u.]	*droop* [%]	Capacitive Limit [MVAr]
19	1.030	5	40.0
21	1.040	2	40.0
30	1.000	2	50.0

TABLE 14. Parameters adopted in the SVC *Q*-Limits smooth modeling for the tutorial system 2 case study.

Sigmoid Switches Slope (*slp*)	$1.5 \cdot 10^7$
Sigmoid Switches Tolerances ($tol_{q,v}^{sup,inf}$)	10^{-10}

This collapse occurs when one of the SVCs reaches its maximum reactive generation capacity, as shown in Figure 6. The system topology and data are available in [30], while the specific parameters for each active SVC are presented in Table 13. It is assumed that each SVC controls its own bus voltage magnitude. This case study considers the static smooth models of SGs and SVCs during simulations, with the sigmoid switch parameters detailed in Table 14.

The CPF analysis revealed that the voltage collapse was caused by the SVC at bus 30 reaching its reactive power generation maximum limit. This collapse is classified as a SNB, which is characterized by the presence of eingenvalues close to zero, as shown in Table 15. Among the four smallest

TABLE 15. IEEE 30-Bus SNB classification of voltage collapse, considering SGs and SVC *Q*-Limits smooth modeling.

Maximum Loadability	138.079297%
Voltage Stability Margin	895.306164737 MW
Reactive Power Generated by $Q_{G_{30},\,svc}$	0.49024314 p.u.
J_R eigenvalues	[(...) 0.000452123879 0.534423518 0.897219043 1.03539813 (...)]

TABLE 16. IEEE 30-Bus modal analysis results.

Eigenvalue (λ^{eig})	Participation Factor
0.000452123879	$Q_{G_1,\,gen} = 96.12\%$, $Q_{G_{19},\,svc} = 1.79\%$, $Q_{G_{21},\,svc} = 1.66\%$, $Q_{G_{30},\,svc} = 0.43\%$
0.534423518	$Q_{G_1,\,gen} = 0.25\%$, $Q_{G_{19},\,svc} = 0.52\%$, $Q_{G_{21},\,svc} = 0.28\%$, $Q_{G_{30},\,svc} = 98.95\%$
0.897219043	$Q_{G_1,\,gen} = 0.38\%$, $Q_{G_{19},\,svc} = 80.46\%$, $Q_{G_{21},\,svc} = 18.95\%$, $Q_{G_{30},\,svc} = 0.2\%$
1.03539813	$Q_{G_1,\,gen} = 2.88\%$, $Q_{G_{19},\,svc} = 19.5\%$, $Q_{G_{21},\,svc} = 76.86\%$, $Q_{G_{30},\,svc} = 0.76\%$

eigenvalues calculated from the matrix J_R, one indicates the SVC at bus 30 as responsible for the voltage collapse in the power system. The other eigenvalues suggest that there are control conflicts between two or more SVCs electrically close to each other. The modal analysis results, shown in Table 16, confirm these findings, with the eigenvalue responsible for the collapse highlighted.

Although the eigenvalue associated with the collapse is not the smallest, it has the highest participation factor. This factor indicates that the SVC at bus 30, which generates the reactive power, is the main cause of the voltage collapse in the system.

V. CONCLUSION

This study comprehensively examines the advantages of the Smooth Power Flow formulation in addressing voltage collapse. By utilizing static methodologies for the reactive power limits of synchronous generators, synchronous condensers, and the static VAr compensators capacity limit, based on the full Newton implementation, the power flow formulation is enhanced. This approach incorporates control equations that accurately depict the behavior of these devices during simulations.

In this paper, sigmoid functions are used to approximate discontinuities in device control equations. These functions introduce smoothness into the traditional power flow formulation without sacrificing precision in the calculation of power flow solutions. The simulation results presented in section IV demonstrate the effectiveness of the proposed approach. The smooth formulation effectively identifies tendencies of SNB bifurcations at the maximum loadability point in EPS voltage stability analyses using CPF. This is a significant improvement over the traditional formulation, which relies on LIB identification. By providing a more accurate and nuanced representation of bifurcation tendencies, the smooth formulation enhances the reliability of voltage stability assessments. Additionally, the results from modal analysis confirm the mathematical findings introduced in [29], providing cross-validation between the two publications.

Future perspectives of this research include applying the proposed new formulation to voltage and small-signal analysis of EPS with uncertainties related to load growth, intermittent power sources, and spinning reserve, among others. Moreover, since the proposed approach only alters the PF formulation (which is the core engine of the CPF calculation), the development of a parallel and distributed version of this approach can also be investigated to further enhance its computational efficiency.

REFERENCES

[1] W. F. Tinney and C. E. Hart, "Power flow solution by Newton's method," *IEEE Trans. Power App. Syst.*, vol. PAS-86, no. 11, pp. 1449–1460, Nov. 1967.

[2] (Feb. 2024). *Supporting LAC Countries in Their Reform Efforts*. International Energy Agency, (IEA). [Online]. Available: https://www.oecd.org/latin-america/countries/

[3] F. D. Freitas, A. C. Santos, L. F. J. Fernandes, and Y. G. I. Acle, "Restarted holomorphic embedding load-flow model based on low-order Padé approximant and estimated bus power injection," *Int. J. Electr. Power Energy Syst.*, vol. 112, pp. 326–338, Nov. 2019.

[4] R. Yao, Y. Liu, K. Sun, F. Qiu, and J. Wang, "Efficient and robust dynamic simulation of power systems with holomorphic embedding," *IEEE Trans. Power Syst.*, vol. 35, no. 2, pp. 938–949, Mar. 2020.

[5] C. Liu, B. Wang, X. Xu, K. Sun, D. Shi, and C. L. Bak, "A multi-dimensional holomorphic embedding method to solve AC power flows," *IEEE Access*, vol. 5, pp. 25270–25285, 2017.

[6] P. Kundur, "Definition and classification of power system stability IEEE/CIGRE joint task force on stability terms and definitions," *IEEE Trans. Power Syst.*, vol. 19, no. 3, pp. 1387–1401, Aug. 2004.

[7] N. Hatziargyriou, J. Milanovic, C. Rahmann, V. Ajjarapu, C. Canizares, I. Erlich, D. Hill, I. Hiskens, I. Kamwa, B. Pal, P. Pourbeik, J. Sanchez-Gasca, A. Stankovic, T. Van Cutsem, V. Vittal, and C. Vournas, "Definition and classification of power system stability—Revisited & extended," *IEEE Trans. Power Syst.*, vol. 36, no. 4, pp. 3271–3281, Jul. 2021.

[8] T. Van Cutsem and C. Vournas, *Voltage Stability of Electric Power Systems*. Cham, Switzerland: Springer, 2007.

[9] C. W. Taylor, *Power System Voltage Stability*. New York, NY, USA: McGraw-Hill, 1994.

[10] P. S. Kundur, *Power System Stability and Control*. New York, NY, USA: McGraw-Hill, 1994.

[11] C. A. Canizares and F. L. Alvarado, "Point of collapse and continuation methods for large AC/DC systems," *IEEE Trans. Power Syst.*, vol. 8, no. 1, pp. 1–8, Feb. 1993.

[12] P. D. P. Salazar, Y. Ilyasov, L. F. C. Alberto, E. C. M. Costa, and M. B. C. Salles, "Saddle-node bifurcations of power systems in the context of variational theory and nonsmooth optimization," *IEEE Access*, vol. 8, pp. 110986–110993, 2020.

[13] V. Ajjarapu and C. Christy, "The continuation power flow: A tool for steady state voltage stability analysis," *IEEE Trans. Power Syst.*, vol. 7, no. 1, pp. 416–423, Feb. 1992.

[14] I. Drovtar, M. Leinakse, K. Tuttelberg, and J. Kilter, "Utilizing demand response in load modelling for voltage and reactive power control studies," *IEEE Trans. Power Syst.*, vol. 40, no. 2, pp. 1389–1400, Mar. 2025.

[15] G. W. Stagg and A. H. El-Abiad, *Computer Methods in Power System Analysis*. New York, NY, USA: McGraw-Hill, 1968.

[16] L. S. Neves, L. F. C. Alberto, and H.-D. Chiang, "Smooth power flow model for unified voltage stability assessment: Theory and computation," *IEEE Trans. Power Syst.*, vol. 37, no. 6, pp. 4579–4589, Nov. 2022.

[17] L. S. Neves, "Fast methods for voltage stability analysis and control selection considering parameter uncertainties," Ph.D. thesis, Graduate Program Elect. Eng. USP-São Carlos, Universidade de São Paulo, 2022.

[18] Y. Song, T. Liu, and Y. Hou, "Voltage stability constrained optimal power flow considering PV-PQ bus type switching: Formulation and convexification," *IEEE Trans. Power Syst.*, vol. 39, no. 2, pp. 3336–3348, Mar. 2024.

[19] J. P. P. Barbosa and J. A. P. Filho, "New methodologies for SVC modeling in the power flow problem based on sigmoid functions," *Electr. Eng.*, vol. 106, no. 1, pp. 971–981, Feb. 2024.

[20] B. Gao, G. K. Morison, and P. Kundur, "Voltage stability evaluation using modal analysis," *IEEE Power Eng. Rev.*, vol. 12, no. 11, p. 41, Nov. 1992.

[21] Y. Kataoka, "A smooth power flow model of electric power system with generator reactive power limits taken into consideration," in *Proc. IEEE Int. Symp. Circuits Syst.*, May 2005, pp. 5286–5289.

[22] L. Zeng, H.-D. Chiang, L. S. Neves, and L. F. C. Alberto, "On the accuracy of power flow and load margin calculation caused by incorrect logical PV/PQ switching: Analytics and improved methods," *Int. J. Electr. Power Energy Syst.*, vol. 147, May 2023, Art. no. 108905.

[23] L. S. Neves, L. F. C. Alberto, and H.-D. Chiang, "A fast method for detecting limit-induced bifurcation in electric power systems," *Electric Power Syst. Res.*, vol. 180, Mar. 2020, Art. no. 106101.

[24] L. S. Neves and L. F. Costa Alberto, "On the computation of the locally closest bifurcation point considering loading uncertainties and reactive power limits," *IEEE Trans. Power Syst.*, vol. 35, no. 5, pp. 3885–3894, Sep. 2020.

[25] J. P. P. Barbosa, "Using sigmoid functions for representing limits of generators and static varcompensators and their impact on the voltage stability study," M.S. thesis, Graduate Program Elect. Eng. (PPEE/UFJF), Juiz de Fora, MG, 2023.

[26] G. K. Morison, B. Gao, and P. Kundur, "Voltage stability analysis using static and dynamic approaches," *IEEE Trans. Power Syst.*, vol. 8, no. 3, pp. 1159–1171, Aug. 1993.

[27] J. A. Passos Filho, N. Martins, and D. M. Falcao, "Identifying power flow control infeasibilities in large-scale power system models," *IEEE Trans. Power Syst.*, vol. 24, no. 1, pp. 86–95, Feb. 2009.

[28] S. Greene, I. Dobson, and F. L. Alvarado, "Contingency ranking for voltage collapse via sensitivities from a single nose curve," *IEEE Trans. Power Syst.*, vol. 14, no. 1, pp. 232–240, Feb. 1999.

[29] L. S. Neves, L. F. C. Alberto, and H.-D. Chiang, "Fast contingency screening for voltage stability analysis considering both SNBs and SIBs," *Electr. Power Syst. Res.*, vol. 213, Dec. 2022, Art. no. 108303.

[30] R. Christie. (1999). *Power Systems Test Case Archive*. [Online]. Available: http://labs.ece.uw.edu/pstca/

[31] L. Chen and Y. Min, "Limit induced bifurcation caused by SVC capacity limit," in *Proc. IEEE Lausanne Power Tech*, Jul. 2007, pp. 250–254.

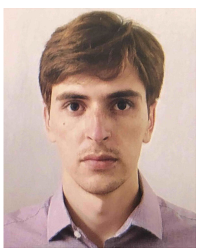

JOÃO PEDRO PETERS BARBOSA (Graduate Student Member, IEEE) received the B.Sc. and M.Sc. degrees in electrical engineering from the Federal University of Juiz de Fora, Juiz de Fora, Brazil, in 2021 and 2023, respectively. He is currently pursuing the D.Sc. degree in electrical engineering with the Department of Electrical Engineering, Engineering School, University of São Paulo, São Carlos, Brazil. His research interests include power system stability analysis and control.

JOÃO ALBERTO PASSOS FILHO (Senior Member, IEEE) received the B.Sc. and M.Sc. degrees from the Federal University of Juiz de Fora (UFJF), Minas Gerais, Brazil, in 1995 and 2000, respectively, and the D.Sc. degree from the Federal University of Rio de Janeiro (COPPE/RFRJ), in 2005. From 1997 to 2009, he was with the Electric Energy Research Center (CEPEL) on developing power system analysis software. Since 2009, he has been with the Department of Electrical Engineering, UFJF. At UFJF, he was the Head of the Department of Electrical Energy for two terms, from 2011 to 2015, where he was the Coordinator of the Graduate Program in Electrical Engineering, in 2019 and 2020. His main research interests include voltage security analysis, optimization, and control of power systems. Additionally, he has been working as an Associate Editor of academic journals IEEE TRANSACTIONS ON SUSTAINABLE ENERGY and IEEE POWER ENGINEERING LETTERS.

RODRIGO ANDRADE RAMOS (Senior Member, IEEE) received the B.Sc., M.Sc., and Ph.D. degrees in electrical engineering from the University of São Paulo, São Paulo, Brazil, in 1997, 1999, and 2002, respectively. He is currently an Associate Professor with the Department of Electrical and Computer Engineering, São Carlos School of Engineering, a unit of the University of São Paulo. He was a Visiting Professor with the University of New South Wales, Sydney, NSW, Australia, and a Visiting Associate Professor with the University of Waterloo, Waterloo, ON, Canada. He was an Associate Editor of IEEE TRANSACTIONS ON SUSTAINABLE ENERGY, IEEE TRANSACTIONS ON SMART GRID, and the *Journal of Modern Power Systems and Clean Energy*.

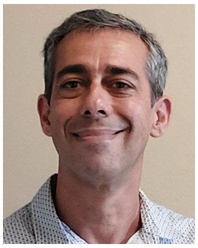

LUÍS FERNANDO COSTA ALBERTO (Senior Member, IEEE) received the M.S. and Ph.D. degrees in electrical engineering from the University of São Paulo (USP), São Carlos, Brazil, in 1997 and 2000, respectively. He is currently a Full Professor with the Electrical Engineering Department, School of Engineering of São Carlos, USP. He held one-year appointments with Cornell University as a Visitor, in 2004 and 2011. He is the co-author (with H.-D. Chiang) of the book *Stability Regions of Nonlinear Dynamical Systems: Theory, Estimation, and Applications* (Cambridge University Press, Cambridge, U.K., 2015). His research interests include analysis of nonlinear circuits and power systems. His contributions include the development of stability theory, stability region theory, invariance principles, and direct methods for stability analysis of power systems. He was a recipient of the Instituto de Engenharia Award as the Best Student of the Engineering School, USP, in 1995.